# Comparison of Divertor Heat Flux Splitting by 3D Fields with Field Line Tracing Simulation in KSTAR

W. Choe[1,2*], K. Kim[1,2], J.-W. Ahn[3], H.H. Lee[4], C.S. Kang[4], J.-K. Park[5], Y. In[4], J.G. Kwak[4], and S.W. Yoon[4]

[1]Korea Advanced Institute of Science and Technology (KAIST), Daejeon, Republic of Korea

[2]Impurity and Edge plasma Research Center, KAIST, Daejeon, Republic of Korea

[3]Oak Ridge National Laboratory, Oak Ridge TN, USA

[4]National Fusion Research Institute, Daejeon, Republic of Korea

[5]Princeton Plasma Physics Laboratory, Princeton NJ, USA

[*]*E-mail contact of main author: wchoe@kaist.ac.kr*

**Abstract.** Non-axisymmetric (3D) magnetic fields in tokamaks form stochastic field layers by opening magnetic islands, leading to modifications of magnetic field structure and heat flux distribution on the divertor. The heat flux splitting pattern strongly depends on the applied field configuration, which is incorporated into 3D perturbed equilibrium. Understanding their physical relations can provide a new insight of divertor heat flux control under the 3D fields and clues for underlying physics of plasma response to the 3D fields. We present experimental and numerical analysis of divertor heat flux spitting by 3D magnetic fields in KSTAR through a dedicated experiment measuring modification of divertor heat flux profile in the n=2 resonant and non-resonant field configurations. The measured heat flux profiles are directly compared to the magnetic field line tracing simulation using POCA-FLT code, which fully considers vacuum and ideal plasma response models. Measurements indicate the 3D fields induce strong splitting of heat flux on the divertor target due to formation of stochastic field layers. Splitting characteristics largely depends on the applied 3D fields and its alignment to the pitch of axisymmetric equilibrium. Modeling of field line connection length shows good agreement with measurements, well reproducing the splitting of heat flux. In particular, simulations with ideal plasma response better reproduce the measured profiles by excitation of non-resonant field components in the non-resonant 0 degree phase and shielding of resonant field components in the resonant 90 degree phase.

## 1. Introduction

Application of toroidally non-axisymmetric (3D) magnetic fields has great impacts on the stability and performance of tokamaks. Suppression or mitigation of edge localized modes by resonant magnetic perturbations (RMP) is one of the best benefits of the 3D fields [1]. Application of non-resonant magnetic fields has great potential for control of toroidal plasma rotation and performance [2]. In addition, there is a side effect of the applied 3D fields, which is the modification of magnetic field topology in the edge-SOL-divertor region. In particular, the applied 3D fields form stochastic field layers at the plasma boundary by opening magnetic islands, consequently leading to splitting of heat flux on the divertor target [3]. The heat flux splitting pattern strongly depends on the applied field configuration, which is incorporated into the 3D perturbed equilibrium. Understanding their physical relations can provide a new insight for divertor heat flux control under the 3D fields and clues for underlying physics of plasma response to the 3D fields.

Field line tracing (FLT) simulation is a useful tool to investigate the formation of stochastic magnetic field structure in the presence of external and/or internal 3D magnetic fields. Given the 3D field structure, a typical FLT code solves a set of magnetic differential equations

$$\frac{\partial R}{\partial \phi} = \frac{RB_R}{B_\phi}, \qquad \frac{\partial Z}{\partial \phi} = \frac{RB_Z}{B_\phi}$$

where $B_R$, $B_Z$, $B_\phi$ are the magnetic fields on the cylindrical coordinates. By tracking the magnetic field lines, the FLT codes provide information of distorted magnetic flux surfaces by 3D fields, such as the field line connection length, the field line loss fraction, the Poincare map at the prescribed toroidal angle, and the magnetic footprint on the divertor plate covering the full toroidal angle.

The formation of the stochastic field layers by 3D fields has been mainly studied using vacuum field approximation that ignores plasma response to the vacuum 3D fields. This approach has been successful to elucidate general observations of magnetic field line splitting and divertor heat flux modification by the 3D fields of high toroidal mode number [3]. However, importance of plasma response physics has been reported in the recent study [4], where numerical FLT analyses compared to experimental observations of magnetic footprint showed that the vacuum fields may not be valid enough and plasma response should be included to explain and reproduce the strong amplification of the applied 3D fields of low toroidal mode number (i.e. n=1). This is because the externally applied 3D fields are generally perturbed and reestablished by the plasma response, which causes strong shielding and amplification of the vacuum 3D fields via alignment with the pitch of axisymmetric equilibrium [5, 6].

In this paper, we investigate the divertor heat flux modification by externally applied 3D magnetic fields in the KSTAR plasmas, depending on the applied 3D field configuration. Dedicated experiment, where non-resonant and resonant n=2 magnetic fields were generated on the time-varying axisymmetric equilibrium, was carried out. Heat flux distributions on the divertor target were measured in the set of 3D field configurations and compared with numerical field line tracing simulations.

## 2. Numerical model

The POCA-FLT code [4, 7] has been utilized to simulate modifications of magnetic field line structure by 3D magnetic fields. Magnetic field line splitting due to 3D fields has been modeled using vacuum and ideal plasma response models in the realistic tokamak geometries including divertor structure for the KSTAR tokamak. The POCA-FLT simulation can fully consider the ideal plasma response by coupled calculation with the IPEC code [8] that shields and amplifies the resonant and non-resonant field components at the rational flux surfaces. Such a capability is important in modeling the stochastic magnetic field structure, since the plasma response plays a crucial role in reestablishing the perturbed 3D equilibrium and forming the stochastic field layers. Instead of adopting additional numerical models for the plasma response, such as helical current sheet model aligned with the external field to represent the screening of the resonant magnetic perturbations, the POCA-FLT employs a full ideal plasma response calculation by the IPEC code.

Divertor heat flux profile measured in the 3D field experiments can be compared with a numerical parameter, the field line connection length (Lc) distributions of magnetic field lines calculated by the POCA-FLT code. The comparison between the heat flux and Lc can be generally accepted on the physical basis that electrons are the main carrier of plasma energy to the divertor and their gyro radii are small enough to approximate the electron orbit

trajectory to the magnetic field line trajectory. Collisional spreading of parallel electron heat transport is ignored in the simulation. Then, the Lc can be a useful parameter to represent the plasma heat transport on the divertor target along the magnetic field lines and provide important information of the magnetic field topology in the boundary area through a comparison with divertor heat flux measurements. For example, larger connection length implies that the field lines stay in the hot plasma core for a longer time to carry higher heat flux to the target. Therefore, Lc contour imitates the heat flux distribution on the target in this study. The field line connection length in the POCA-FLT is calculated by tracking magnetic field lines for 200 toroidal turns in co-Ip and counter-Ip directions until the field lines touch the plasma facing components.

Fig. 1 presents an example of typical Lc contours for the KSTAR plasma obtained from the POCA-FLT simulation, which show footprint of magnetic field lines and lobe structures on the divertor target under n=2 fields. Heat flux striation patterns with vacuum fields and ideal plasma response are compared to clarify the role of ideal plasma response in this simulation. Here, n=2 fields were generated only using middle IVCCs in KSTAR, therefore the applied 3D fields were largely non-resonant and the axisymmetric field pitch represented by q-profile has less effects on the plasma response than the cases fully employing all of three rows of IVCCs. The Lc contours from the simulation show that strong striations on the divertor plate can be produced by vacuum 3D fields but they are largely shielded by ideal plasma response. In the ideal plasma case, resonant field components opening magnetic islands in the vacuum fields were significantly shielded by the ideal plasma, while overall shape of the striation patterns was not changed compared to the vacuum field calculations.

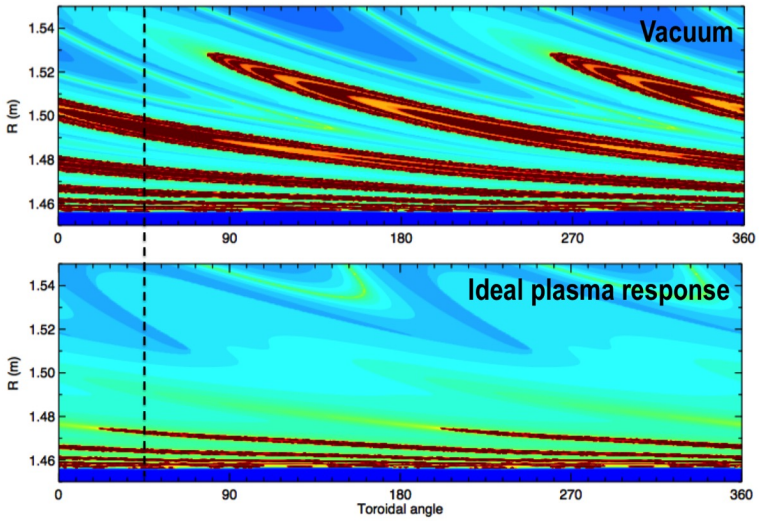


*Figure 1. Striation patterns of divertor heat flux modified by n=2, 3D fields using middle IVCCs. Divertor footprints are represented by connection length calculated by POCA-FLT. Vertical dashed line indicates the toroidal angle for comparison of heat flux in Fig. 2.*

Fig. 2 is a comparison of heat flux measurement by divertor IRTV system in KSTAR [9] with the POCA-FLT simulations for the case in Fig. 1, which presents the normalized heat flux profile against the normalized Lc profiles calculated with the vacuum fields and ideal plasma response model. In this relatively simple case using middle IVCCs, the POCA-FLT simulations well reproduce the heat flux splitting on the target with the connection length profiles, while their agreement depends on the plasma response model used. One can observe in Fig. 2 that a second peak was produced by the applied 3D fields due to the formation of stochastic field layers in the boundary area (black). This second peak is well reproduced by

the simulation using vacuum fields, however strong third peak is also predicted due to the existence of stronger field line splitting than the measurements (green). On the other hand, when ideal plasma response is used, the field line tracing simulation shows complete shielding of the third peak of the vacuum fields, and the second peak is also strongly shielded such that the peak appears weak compared to those in the vacuum field and the measurement (red). The broadened peaks of the heat flux measurement may be due to finite orbit width of particles carrying heat onto the target and collision of such particles striking the target, which are not included in the simulation. One can also notice that the selection of a plasma response model will be important for better comparison as plasmas in reality are non-ideal and lie somewhere between ideal and vacuum plasma regimes.

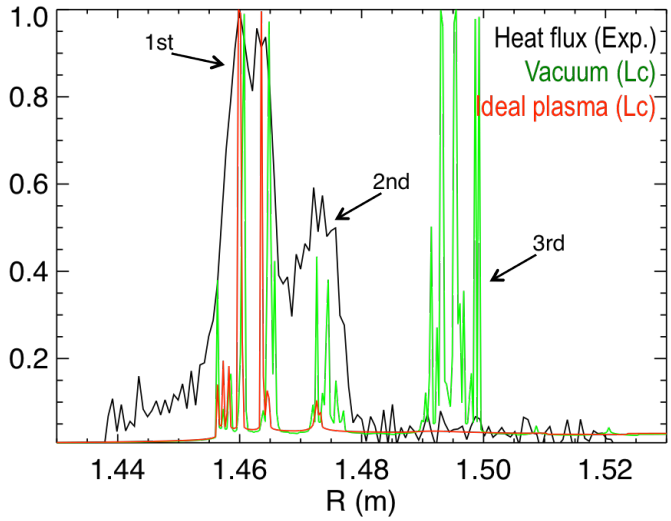


*Figure 2. Comparison of heat flux profiles with connection length (Lc) profiles by POCA-FLT with vacuum field and ideal plasma response models. Profiles were normalized to the maxima.*

## 3. Experimental observations

A dedicated experiment has been carried out in the KSTAR tokamak, which measures divertor heat flux distributions and scans the heat flux profile with relative phase of 3D magnetic field coils. AC waveforms were used in the single discharge to produce time varying spectrum of 3D fields that continuously changed alignment with the equilibrium pitch. Two distinctive phases of n=2 fields, resonant +90 degree phase and non-resonant 0 degree phase shown in Fig. 3, were examined in the discharge. The pitch-alignment in the axisymmetric equilibrium was scanned with $q_{95}$ by increasing plasma current from 500 kA to 750 kA to vary $q_{95}$ from 4.9 to 3.6, accordingly. The time history of this discharge is presented in the Fig. 4, showing the evolution of operational and kinetic plasma parameters.

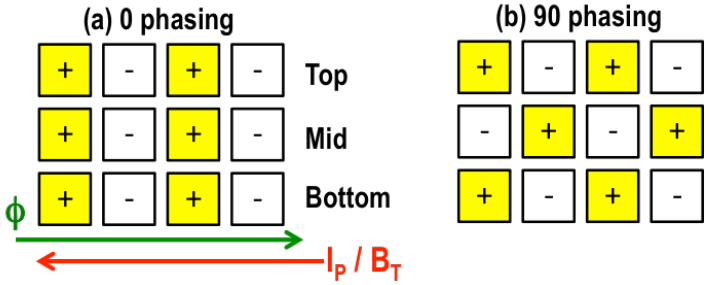


*Figure 3. n=2 IVCC configurations in KSTAR for (a) 0 phasing and (b) 90 phasing*

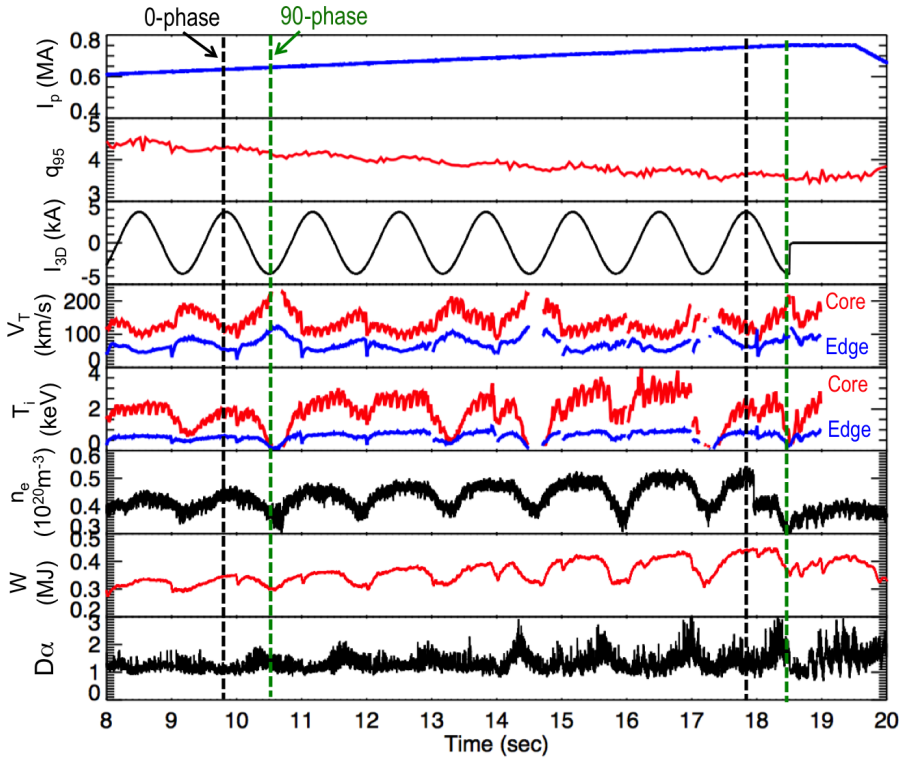


*Figure 4. Time history of the 3D field experiment, which measures divertor heat flux distribution depending on the relative coil phase and $q_{95}$. From top to bottom, plasma current, $q_{95}$, currents of 3D field coil, toroidal rotation, ion temperature, electron density, stored energy, and Dα are presented as a function of discharge time.*

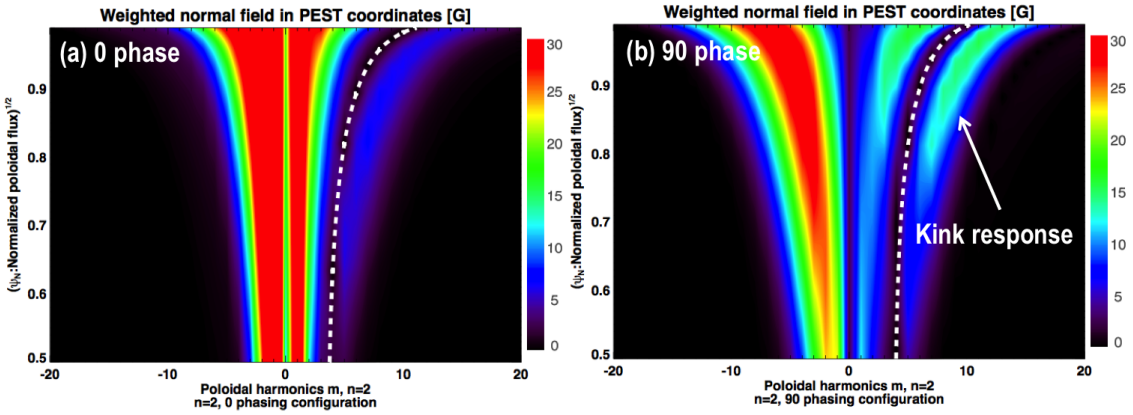


*Figure 5. Poloidal field spectrum with ideal plasma response for (a) 0 and (b) 90 phase*

One can notice that resonant-type plasma responses came out as the phase is changed from non-resonant phase to resonant phase (black → green) along with reduction of plasma density by enhanced particle transport. Ion temperature was also decreased, and thereby energy confinement was degraded during the period of resonant field phase. On the other hand, toroidal rotation was increased during the same period similarly with the typical RMP experiments, while no clear changes in ELM behavior was observed. In the period where the coil phase changed from the resonant phase to the non-resonant phase, plasma responses appeared the opposite way. These distinct features of the resonant and non-resonant plasma response are consistently found in the calculation of poloidal field spectrum with ideal plasma response for each phase, as shown in Fig. 5. One can notice that very strong excitation of

kink-type plasma response in the 90 phase is predicted by ideal plasma response, while the pitch-aligned resonant components are largely shielded. Such shielding and excitation appear weaker in the non-resonant 0 phase. As $q_{95}$ decreased, the resonant plasma response was observed to become stronger due to the significant pitch-alignment of the applied 3D fields with axisymmetric equilibrium.

## 4. Comparison of heat flux profiles between experiment and modeling

Fig. 5 presents the contours of magnetic field line connection length obtained from the POCA-FLT code with vacuum field and ideal plasma response, showing the striation patterns on the divertor for each phase at $q_{95}$~4.3. One can find that the resonant 90 degree phase produces much stronger splitting of magnetic field lines than the non-resonant 0 degree phase. The ideal plasma response weakens the splitting by shielding of resonant field components of the applied fields in both of 0 and 90 degree phases. One can find such shielding effects are more significant for the 90 degree phase, while the shielding was weak for the non-resonant 0 degree phase. As similarly shown with the modeling results in Fig. 1, overall shapes of the striation pattern for each phase are not significantly changed by the plasma response.

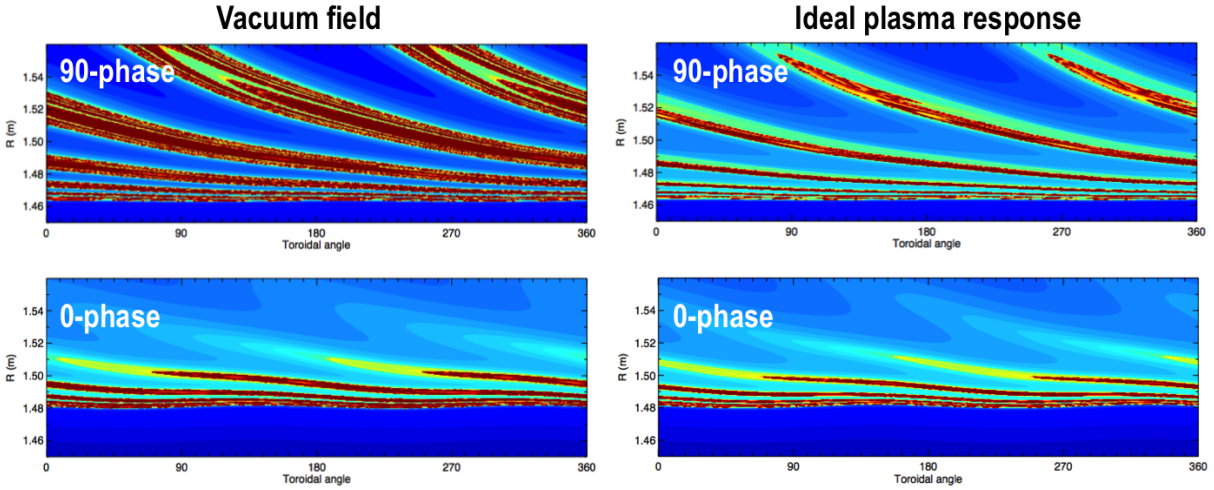


*Figure 6. Striation patterns on the divertor plate for 90 and 0 degree phases, calculated with vacuum field and ideal plasma response.*

For detailed comparison of heat flux profiles between measurement and modeling, we select two time-periods indicated by vertical dashed lines in Fig. 4, where the axisymmetric equilibrium was changed by ramp-up of plasma current. Therefore, $q_{95}$ of ~4.3 and ~3.6 was achieved at t~10s and t~18s, respectively. The POCA-FLT simulations have been performed using 0 and 90 degree phase for each $q_{95}$ value and thereby for different axisymmetric equilibrium, and compared with heat flux profiles measured by the divertor IRTV. Fig. 6 presents the heat flux profiles of measurement and simulation result with vacuum and ideal plasma response models at a selected toroidal angle ($\phi$=45°).

One can find from both of measurements and simulations that splitting of heat flux and Lc profiles are stronger in the non-resonant 0 phase than the resonant 90 phase. Three peaks were clearly generated by the 0 phase, while only two peaks appeared clear in the 90 phase. One can also find that in the 0 phase cases, the baseline of Lc profiles were significantly increased by ideal plasma response. The third peak in the outer divertor region that was not captured by vacuum field was reproduced by the ideal plasma calculation, which much better agrees with the measurement. This is due to the excitation of non-resonant field components by the plasma response that are not aligned to the pitch of axisymmetric equilibrium. However, in

the 90 phase cases, the Lc peaks were largely mitigated by ideal plasma response compared to the vacuum field, due to shielding of the pitch-aligned resonant field components. In the 90 phase, the ideal plasma response calculations show weaker third peak than the vacuum field, which results in better reproduction of the largely broaden third peak of the measurement in the outer radius on the divertor target. Agreements between the measurement and the calculation in the 90 degree phase appear relatively poor compared to that of 0 degree phase, which implies the ideal plasma response model may not be sufficiently good to explain such a strong plasma response.

Overall, the Lc profiles in the POCA-FLT simulations are in the reasonable agreements with the measurements of modification of divertor heat flux. In particular for the 0 degree phase, simulations with ideal plasma response predict measured third peaks (a, c) that not produced by vacuum field calculations. Two other peaks are in very good agreements. However, for 90 degree phase cases, third peaks predicted by both ideal plasma and vacuum fields were very weak in the measurements in spite of good agreements of the other two main peaks. One may note that even in the disagreement of the third peak in the 90 phase, ideal plasma response model indicates weaker third peak than the vacuum fields due to the shielding of kink-excitation, which is more consistent to the experimental observations.

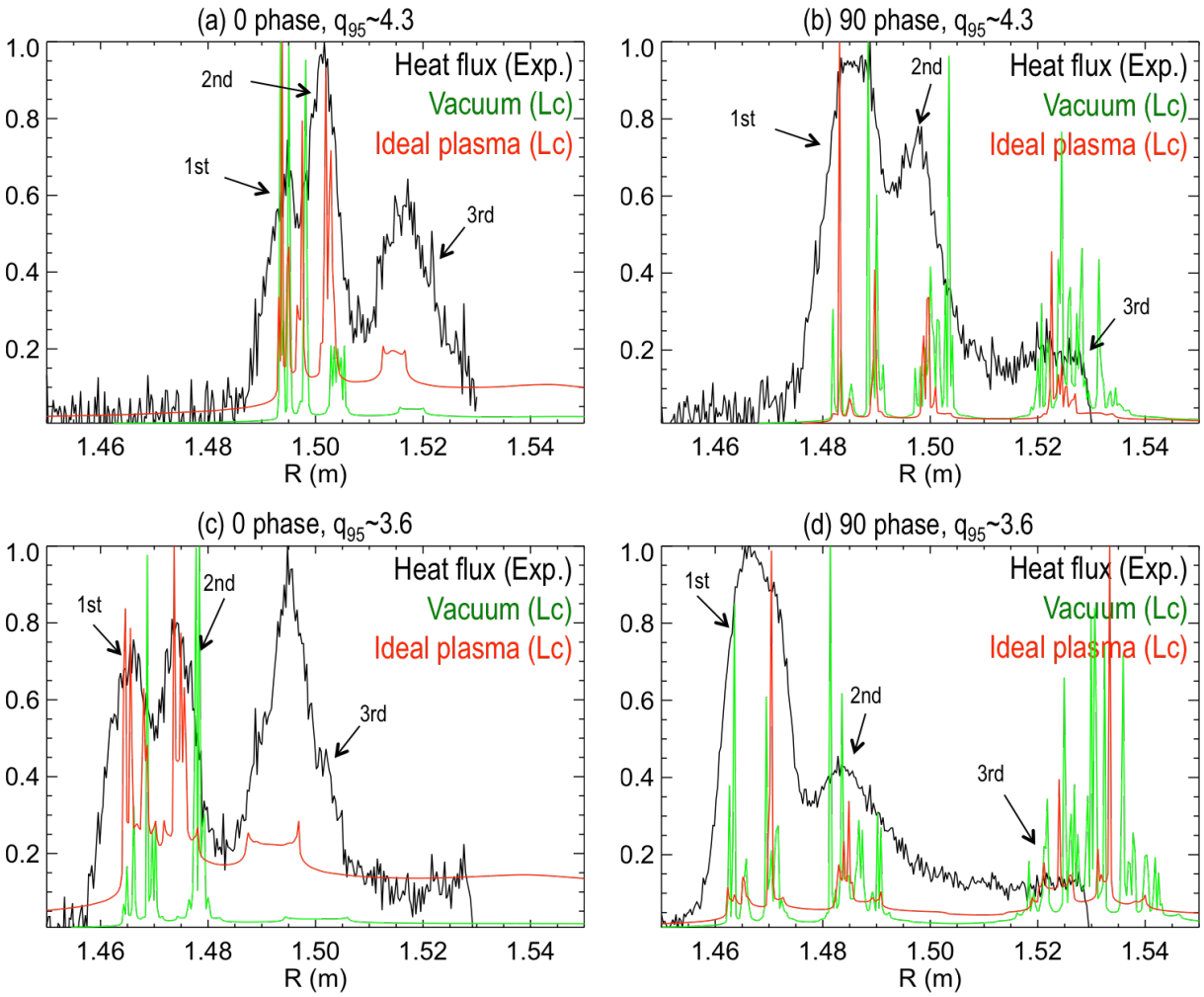


*Figure 7. Comparison of heat flux profiles between measurements and POCA-FLT simulations, considering vacuum field and ideal plasma response. Two 3D field phases (0 and 90) for high $q_{95}$ (~4.3) and low $q_{95}$ (~3.6) are presented.*

## 5. Summary

We present the comparison of divertor heat flux splitting by 3D magnetic fields in KSTAR with field line tracing simulation using the POCA-FLT code. Experimental observations of plasma response to the resonant and non-resonant 3D field configurations are consistently found in the 3D perturbed equilibrium calculations. The field line connection length in the POCA-FLT well reproduces the measured divertor heat flux profile with the ideal plasma response model rather than the vacuum fields. The excitation of kink response and shielding of pitch-aligned resonant field components by the ideal plasma response consistently explain the splitting of the divertor heat flux for resonant and non-resonant configurations. The consistency between measurement and calculation is relatively poor for the strong resonant 90 degree phase. General plasma response physics model will be a key to achieve better understanding of divertor heat flux modifications due to the application of 3D magnetic fields in tokamaks, especially for the case with significant perturbed 3D field equilibrium.

## Acknowledgements

This work is supported by National Research Foundation of Korea (NRF) funded by the Ministry of Science, ICT and Future Planning (NRF-2014M1A7A1A03045092), and the Korean Ministry of Science, ICT and Future Planning under the KSTAR project contract (NFRI).

## References

[1] EVANS, T.E., et al., “Suppression of large edge-localized modes in high-confinement DIII-D plasmas with a stochastic magnetic boundary”, Phys. Rev. Lett. **92** (2004) 235003.

[2] KIM, K., et al., “Calculation of neoclassical toroidal viscosity with a particle simulation in the tokamak magnetic braking experiments”, Nucl. Fusion **54** (2014) 073014.

[3] AHN, J.-W., et al., “Characterization of divertor footprints and the pedestal plasmas in the presence of applied n = 3 fields for the attached and detached conditions in NSTX”, Plasma Phys. Control. Fusion **56** (2014) 015005.

[4] KIM, K., et al., “Ideal plasma response to vacuum magnetic fields with resonant magnetic perturbations in non-axisymmetric tokamaks”, Plasma Phys. Control. Fusion **57** (2015) 104002.

[5] BOOZER, A.H., “Error Field Amplification and Rotation Damping in Tokamak Plasmas”, Phys. Rev. Lett. **86** (2001) 5059.

[6] TURNBULL, A.D., et al., “Comparisons of linear and nonlinear plasma response models for nonaxisymmetric perturbations”, Phys. Plasmas **20** (2013) 056114.

[7] KIM, K., et al., “δf Monte Carlo calculation of neoclassical transport in perturbed tokamaks”, Phys. Plasmas **19** (2012) 082503.

[8] PARK, J.-K., et al., “Computation of three-dimensional tokamak and spherical torus equilibria”, Phys. Plasmas **14** (2007) 052110.

[9] LEE, H.H., et al., “Divertor infrared thermography system on KSTAR”, KSTAR Conference (2015), Daejeon, Korea.